Orclever Proceedings of Research and Development
https://doi.org/10.56038/oprd.v2i1.239
OR CLEVER Science & Research Group

Conference Article

Classification of 3D-DWT Features of Brain Tumours with SVM

Mucahid Barstugan[1*]

[1] Konya Technical University, Engineering and Natural Sciences Faculty, Electrical and Electronics Engineering, 0000-0001-9790-5890, mbarstugan@ktun.edu.tr
* Correspondence: mbarstugan@ktun.edu.tr; +90 541 694 55 72

(First received January 6, 2023 and in final form March 12, 2023)

3rd International Conference on Access to Recent Advances in Engineering and Digitalization
March 15 - 17, 2023

Reference: Classification of 3D-DWT Features of Brain Tumours with SVM. Orclever Proceedings of Research and Development,2(1), 39-49

Abstract

Brain tumours are one of the most challenging medical conditions to diagnose and treat. Accurate and timely classification of brain tumours is critical for effective treatment planning and patient management. Machine learning algorithms have shown great promise in improving the accuracy of brain tumour classification. This study implemented high-grade glioma (HGG) and low-grade glioma (LGG) classification on four different 3D-MRI (magnetic resonance imaging) scans (FLAIR, T1, T1c, T2). By using four different scans, 15 different combinations were created for classification process. 3D Discrete Wavelet Transform was used to transform tumour images for feature extraction stage. 36 different wavelet types were used for image transformation. First Order Statistics (mean, variance, kurtosis, skewness, entropy, energy) were extracted from transformed images of 36 wavelet types. Support Vector Machines (SVM) algorithm classified the FOS features that were obtained on BraTS 2017 dataset. The 2-fold, 5-fold, and 10-fold cross-validations are implemented and six metrics (sensitivity, specificity, accuracy, precision, F1-score, AUC) evaluated the performance of proposed method. Consequently, proposed method achieved remarkable scores of 95.23% (sensitivity), 78.81% (specificity), 90.89% (accuracy), 92.59% (precision), 93.89% (F1-score), and 87.02% (AUC) for HGG/LGG classification of 3D brain MRI data on T1+T1c+T2 combination by 2-fold cross validation.

Keywords: 3D brain MRI data, BraTS2017, Binary Classification, Brain tumour, Feature Extraction

https://doi.org/10.56038/oprd.v2i1.239

1. Introduction

Brain tumours are abnormal growths of cells in the brain. They can be either malignant (cancerous) or benign (non-cancerous) and can arise from different types of cells in the brain, such as astrocytes, oligodendrocytes, or ependymal cells. Brain tumours can cause a variety of symptoms, depending on their location, size, and type. These symptoms can include headaches, seizures, vision or hearing problems, cognitive changes, and difficulty with balance and coordination. Treatment for brain tumours may include surgery, radiation therapy, chemotherapy, or a combination of these approaches. The prognosis for brain tumours varies widely depending on their type, location, and stage. A glioma (brain tumour) stems from the glial cells in the brain and spine. Grade III and grade IV tumours are considered invasive and defined as a high-grade glioma (HGG), yielding an adverse prognosis. Grades I and grade II tumours are non-invasive and defined as low-grade glioma (LGG), yielding a favourable prognosis [1-4].

The first step in HGG/LGG classification is to label or segment brain tumours. Many studies in the literature have been conducted for the HGG and LGG classification of segmented tumours. [5] extracted features using 3D-GLCM from manually segmented tumour images and classified the extracted features using their proposed methods. They used feature ranking methods on the phase combinations they created during the classification process. Artificial Neural Networks method, which used three different optimization processes based on PSO, was used in the classification stage. The results obtained in the study, which included 210 HGG and 75 LGG images from the BraTS 2017 dataset, were evaluated. In [6], a fusion process was proposed to combine the structural and tissue information of four MRI sequences (T1C, T1, Flair, and T2) for the purpose of brain tumour classification. Four different MRI sequences were combined to obtain a single image, and Discrete Wavelet Transform (DWT) was applied to the obtained image. After the fusion process, the noise was removed by applying the partial differential diffusion filter (PDDF), and the tumour area was obtained by thresholding the noise-removed image. The obtained tumour area was classified by a Convolutional Neural Network (CNN) model. The proposed method was tested on five publicly available datasets, namely BRATS 2012, BRATS 2013, BRATS 2015, BRATS 2013 Leaderboard, and BRATS 2018 datasets, and the results were evaluated. In [7], shape-based HOG, texture-based SFTA and LBP feature sets were extracted from the images to classify tumour images. The extracted features were merged, and an entropy-based feature selection process was performed on a single feature set. The proposed method was tested on the

https://doi.org/10.56038/oprd.v2i1.239

BRATS 2013, BRATS 2014, and BRATS 2015 datasets, and the results obtained were evaluated. Many data are required to apply deep learning methods to brain tumour images. For this purpose, [8] used data augmentation methods. VGG16, ResNet50, and AlexNet models were used to extract features from the created new dataset. The extracted features were classified by SVM. The results obtained in the study conducted on the BraTS 2015 dataset were evaluated. In [9], an active deep learning-based feature selection approach was proposed to segment and recognize brain tumours. First, a clarity map was obtained by applying contrast enhancement to the image, and then the image was transformed into binary form using simple thresholding. In the classification stage, the Inception V3 model was used for deep feature extraction. They simply combined these features with dominant rotated LBP (DRLBP) for better texture analysis and performed the classification process by optimizing the combined vector with the particle swarm optimization (PSO) method. The proposed method was tested on the BraTS 2017 and BraTS 2018, and the results were evaluated.

In this paper, phase combinations, 3D-feature extraction, and binary classification are processed together to create various frameworks to obtain an appropriate model for brain tumour classification on 3D MRI tumour volumes. Six features generated from the FOS are obtained from all MRI phases (FLAIR, T1, T1c, and T2). Four single phases and eleven phase combinations (15 combinations) are considered to find the combination that best represents the data.

The paper is organised as follows. The 3D-DWT transform, feature extraction method, and binary classifier are presented in Section 2. The proposed method is discussed in Section 3. The proposed framework and a literature comparison are examined in Section 4.

2. Materials and Methods

The used data is obtained from the 2017 database from the multimodal brain tumour image segmentation (BraTS) challenge [25–27]. The BraTS2017 training data includes 210 HGG and 75 LGG subjects for which the MR modality is obtained on T1c, FLAIR, T1, and T2 sequences. Each modality includes 155 slices, for a total of 620 slices per patient. Each slice is attained with a 240 × 240 image size and 1-mm slice thickness. In all images, non-brain structures have been labelled by expert board-certified neuroradiologists [10-12].

Figure 1 presents HGG and LGG type tumours, for which tumour size and shape can vary. As shown in Figure 1, the same type of tumours can have different size and shape features, also HGG and LGG type tumours containing different intensities.

https://doi.org/10.56038/oprd.v2i1.239

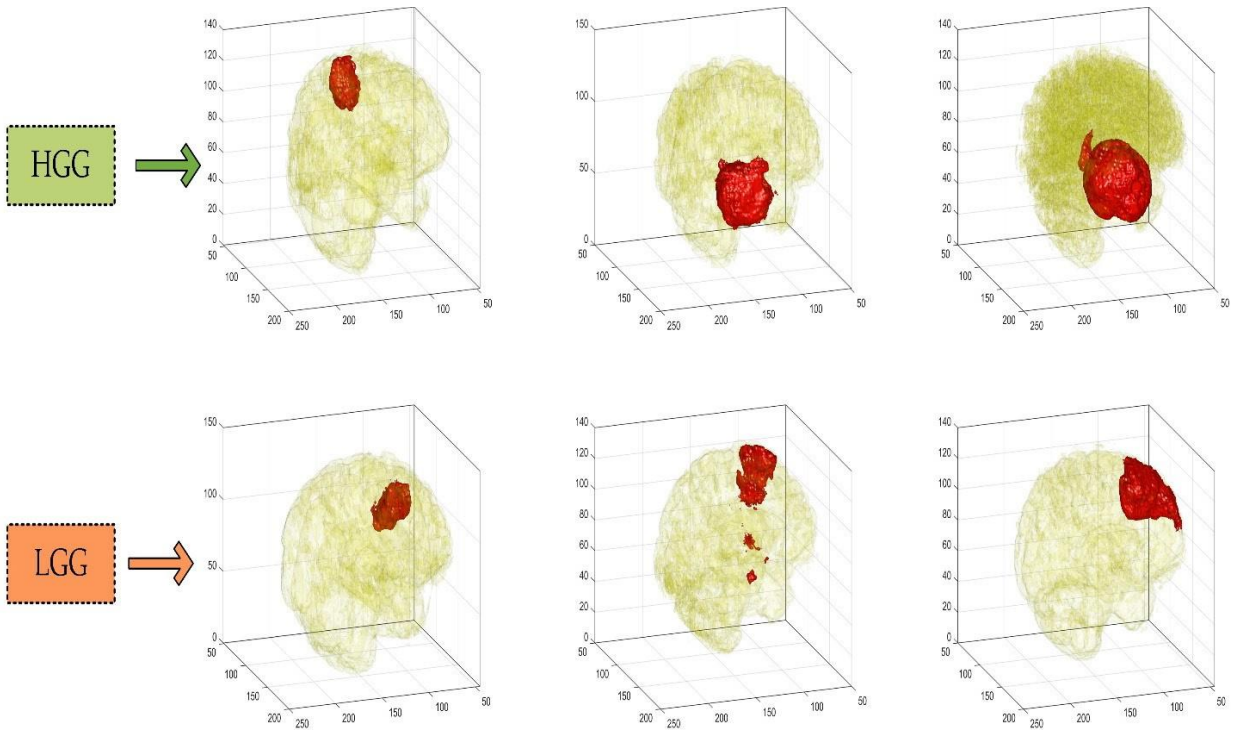

Figure 1: HGG and LGG type tumours in different features

These similarities/differences prevent accurate classification. This study analysed 36 different wavelet types and 15 phase combinations to obtain appropriate framework for accurate classification.

2.1. 3D-DWT Feature Extraction

One dimensional DWT is a multiresolution mathematical tool that separates a signal into approximation (low-pass bands) and detail coefficients (high-pass bands). At the basis of the three-dimensional discrete wavelet transform is the application of the 1B wavelet transform to the three directions x, y, z. 3D DWT includes one scaling function as defined and seven wavelet function as defined. Each 3D function is defined as combinations of 1D functions and mathematical expressions are defined in Equations 1-7.

$$\varphi(x,y,z) = \varphi(x)\varphi(y)\varphi(z) \quad (1)$$

$$\omega^1(x,y,z) = \varphi(x)\omega(y)\varphi(z) \quad (2)$$

$$\omega^2(x,y,z) = \varphi(x)\omega(y)\varphi(z) \quad (3)$$

$$\omega^3(x,y,z) = \omega(x)\omega(y)\varphi(z) \quad (4)$$

$$\omega^4(x,y,z) = \varphi(x)\varphi(y)\omega(z) \quad (5)$$

$$\omega^5(x,y,z) = \omega(x)\varphi(y)\omega(z) \quad (6)$$

https://doi.org/10.56038/oprd.v2i1.239

$$\omega^6(x,y,z) = \varphi(x)\omega(y)\omega(z) \quad (7)$$
$$\omega^7(x,y,z) = \omega(x)\omega(y)\omega(z)$$

The mathematical representation of a three-dimensional signal f(x,y,z) in terms of detail W^{ii} and approximation coefficients W is defined as in Equation 8 (P: Decomposition Level, LMN: 3D Volume) [13].

$$ff(x,y,z) = \frac{1}{\sqrt{LMN}} \sum_l \sum_m \sum_n W_\varphi(P,l,m,n)\varphi_{P,l,m,n}(x,y,z) + \frac{1}{\sqrt{LMN}} \sum_{ii=1}^{7} \sum_{p=1}^{P} \sum_l \sum_m \sum_n W_\omega^{ii}(p,l,m,n)\omega^{ii}_{p,l,m,n}(x,y,z) \quad (8)$$

$$\varphi_{P,l,m,n}(x,y,z) = 2^{\frac{P}{2}}\varphi(2^P x - l, 2^P y - m, 2^P z - n) \quad (9)$$

$$\omega^{ii}(x,y,z) = 2^{\frac{P}{2}}\omega^{ii}(2^P x - l, 2^P y - m, 2^P z - n), ii = \{1,2,\dots,7\} \quad (10)$$

$$W_{p,l,m,n}(P,l,m,n) = \frac{1}{\sqrt{LMN}} \sum_{x=0}^{L-1}\sum_{y=0}^{M-1}\sum_{z=0}^{N-1} ff(x,y,z)\varphi_{P,l,m,n}(x,y,z) \quad (11)$$

$$W_\varphi^{ii}(p,l,m,n) = \frac{1}{\sqrt{LMN}} \sum_{x=0}^{L-1}\sum_{y=0}^{M-1}\sum_{z=0}^{N-1} ff(x,y,z)\omega^{ii}_{P,l,m,n}(x,y,z), ii = \{1,2,\dots,7\} \quad (12)$$

The 3D image is divided into eight sub-bands with low and high pass filters to obtain 3D-DWT coefficients. A 3D image is first filtered by *L(x,y,z)* low pass and *H(x,y,z)* high pass filters in the x direction. The same process is then performed in the y and z directions, respectively, to complete the process. As a result of this all process, eight sub-bands are obtained defined as LLL, LLH, LHL, LHH, HLL, HLH, HHL and HHH. If more separation is desired, more coefficients can be obtained by continuing all process from the LLL coefficients [14]. Figure 2 shows an architectural model that obtains 3D-DWT coefficients using a three-dimensional image of *f(x, y, z)*.

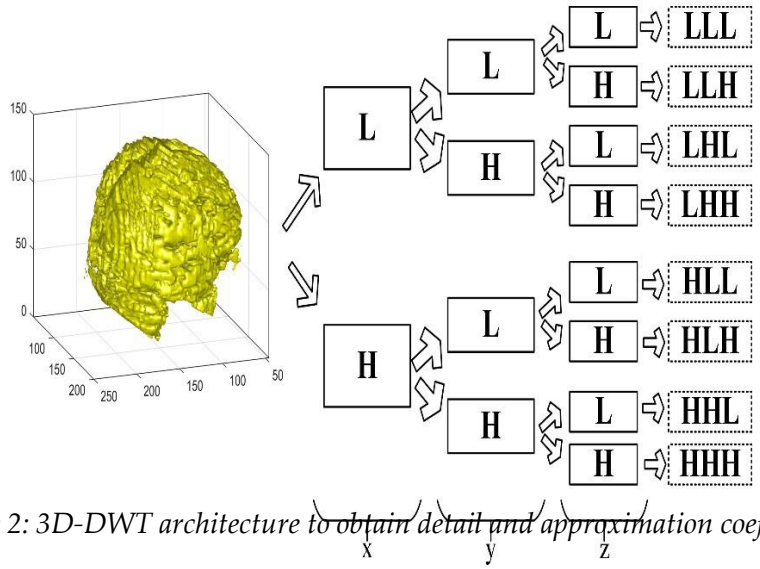

Figure 2: 3D-DWT architecture to obtain detail and approximation coefficients

https://doi.org/10.56038/oprd.v2i1.xxx

The feature set was created by LLL, LLH, LHL, LHH, HLL, HLH, HHL, and HHH coefficients after 3D-DWT. The *mean*, *variance*, *kurtosis*, *skewness*, *entropy*, and *energy* (Equations 13-18) of features [15, 16] were calculated from the coefficients.

Notation:

$$Mean\ (\mu) = \frac{1}{N}\sum^{N}_{ii=1} I_{ii} \quad (13)$$

$$Variiance\ (\sigma^2) = \sum\frac{(I-\sigma)^2}{N} \quad (14)$$

$$Kurtosiis = \frac{1}{N}\sum_{ii=1}^{N}\frac{(I_{ii}-\bar{I})^4}{\sigma^4} \quad (15)$$

$$Skewness = \frac{1}{N}\sum_{ii=1}^{N}\frac{(I_{ii}-\bar{I})^3}{\sigma^3} \quad (16)$$

$$Entropy = -sum(k.* log2(k)) \quad (17)$$

$$Energy = \sum_{ii=1}^{K}\sum_{ii=1}^{M} I_{iiii} \quad (18)$$

where I, σ, N, k, K, and M are image, standard deviation, number of samples, histogram of image, and number of rows and columns, respectively.

During the feature extraction process with 3D-DWT, wavelet types of *db1*, *db2*, *db3*, *db4*, *db5*, *db6*, *db7*, *db8*, *db9*, *coif1*, *coif2*, *coif3*, *coif4*, *coif5*, *sym1*, *sym2*, sym3, *sym4*, *sym5*, *sym6*, *sym7*, *sym8*, *bior1.3*, *bior1.5*, *bior2.2*, *bior2.4*, *bior2.6*, *bior2.8*, *bior3.1*, *bior3.3*, *bior3.5*, *bior3.7*, *bior3.9*, *bior4.4*, *bior5.5*, and *bior6.8* were used.

2.2. Support Vector Machines

SVM is a learning method, which gives high classification accuracy in many applications. An SVM is based on two ideas. The first idea is to map feature vectors to a high dimensional space with a nonlinear method and to use linear classifiers in this new space. The second idea is to find a hyperplane, which separates the data with a high margin. This plane is the best plane, which can separate the data as well as possible [17].

3. Result

In this study, FLAIR, T1, T1c, and T2 phase images were subjected to image transformation with 36 different wavelets. Six features were extracted from each transformed image, and a feature set was obtained for each phase. 15 different combinations were created from the obtained feature sets. The created combinations were classified using 2-fold, 5-fold, and 10-fold cross-validation. The classification stage was divided into two as preliminary classification and final classification. During the classification stage, system performance was evaluated using sensitivity (SEN),specificity

https://doi.org/10.56038/oprd.v2i1.xxx

(SPE), accuracy (ACC), precision (PRE), F1-score, and Area Under Curve

https://doi.org/10.56038/oprd.v2i1.239

(AUC) evaluation metrics given in Equations 19-24. TP, TN, FP, and FN represent the True Positive, True Negative, False Positive, False Negative values, respectively.

$$\text{Sensitivity} = TP / (TP+FN) \quad (19)$$

$$\text{Specificity} = TN / (TN+FP) \quad (20)$$

$$\text{Accuracy} = (TP + TN) / (TP + TN + FN+FP) \quad (21)$$

$$\text{Precision} = TP / (TP+FP) \quad (22)$$

$$\text{F-score} = (2*TP)/(2*TP+FP+FN) \quad (23)$$

$$\text{AUC} = \frac{1}{mn} \sum_{ii=1}^{m} \sum_{ii=1}^{n} 1_{p_{ii>}p_{jj}} \quad (24)$$

3.1. Preliminary classification process

At the preliminary classification stage, 15 different combinations were classified using SVM from feature sets obtained after 36 different wavelet transformations. The best classification results obtained for each combination are presented in the Table 1.

Table 1: The best classification results for each combination

Com-bination	Data	Wavelet Type	k-fold	Metrics (%) (mean ± std)					
				SEN	SPE	ACC	PRE	F-score	AUC
Single	FLAIR	coif1	10	100	5,71±9,9	75,13±3,5	74,83±3,1	85,57±1,9	52,85±4,9
Single	T1	bior4.4	10	100	5,71±9,9	75,13±3,5	74,83±3,1	85,57±1,9	52,85±4,9
Single	T1c	sym1	10	93,33±4,6	45,71±18,1	80,73±3,6	83,09±5,1	87,72±2,2	69,52±7,7
Single	T2	bior3.1	5	97,62±2,4	25,33±8,7	78,59±1,5	78,59±1,6	87,05±0,8	61,47±3,5
Double	FLAIR + T1	bior3.5	2	100	22,65±1,4	79,65±0,1	78,35±5,1	87,87±2,3	61,35±10,5
Double	FLAIR + T1c	sym1	10	90,48±7,1	52,14±22,7	80,39±6,5	84,61±6,8	87,15±4,4	71,3±10,6
Double	FLAIR + T2	db2	5	96,67±1,3	33,33±8,9	80±2,1	80,39±1,8	87,67±1,1	65±4,2
Double	T1 + T1c	bior3.1	2	93,81±4,7	64,04±4,9	85,95±2,1	97,98±1,1	90,75±1,6	78,92±0,1
Double	T1 + T2	db1	2	93,33±1,3	49,35±2,8	81,75±1,9	83,76±1,2	88,28±1,2	71,34±2,1
Double	T1c + T2	db1	2	95,23	65,5±18,2	87,38±4,9	88,66±5,5	91,79±2,9	80,37±9,1
Triple	T1 + T1c + T2	sym1	2	94,76±0,6	77,34±1,4	90,17±0,1	92,13±0,6	93,42±0,1	86,05±0,4
Triple	FLAIR + T1 + T1c	db1	2	92,85±2,1	74,78±12,7	88,08±4,9	91,18±4,3	92±3,2	83,82±7,4
Triple	FLAIR + T1 + T2	sym2	5	94,76±3,1	45,33±10,9	81,75±3,4	82,99±2,8	88,44±2,1	70,04±5,4
Triple	FLAIR + T1c + T2	sym1	10	93,33±5,6	65,35±12,5	85,96±5,5	88,53±4,1	90,7±3,8	79,34±7,1
Quadruple	FLAIR + T1 + T1c + T2	bior3.1	5	93,33±3,5	77,33±10,1	89,12±2,3	92,21±3,1	92,66±1,5	85,33±4,2

https://doi.org/10.56038/oprd.v2i1.239

Table 1 indicates that the best classification result was achieved as 90.17% with 2-fold cross-validation classification on the T1+T1c+T2 combination using the "sym1" wavelet. When other combinations in the Table 1 are examined, it is seen that the type of wavelet varies. The wavelet types that yielded the best results in all experiments are presented in the Table 2.

Table 2: The wavelet types for each combination

Combination	2-fold	5-fold	10-fold
FLAIR	bior3.3	bior3.3	coif1
T1	db1	db1	bior4.4
T1c	db1	db1	sym1
T2	sym1	bior3.1	db1
FLAIR + T1	bior3.5	db1	sym1
FLAIR + T1c	db1	db1	sym1
FLAIR + T2	bior1.3	db2	bior3.3
T1 + T1c	bior3.1	bior3.1	bior3.1
T1 + T2	db1	sym1	bior2.2
T1c + T2	db1	sym1	db1
T1 + T1c + T2	sym1	sym1	sym1
FLAIR + T1 + T1c	db1	sym1	sym1
FLAIR + T1 + T2	db2	sym2	sym1
FLAIR + T1c + T2	sym1	db1	sym1
FLAIR + T1 + T1c + T2	sym1	sym1	bior3.1

Table 2 presents that the “db1”, “sym1”, and ”bior type” are the most effective wavelets for 3D-MRI brain data. These wavelets transform the images with keeping the significant features.

3.2. Final classification process

At the final classification stage, the phase combination, wavelet type, and cross-validation type obtained in the preliminary classification stage were used. SVM classification was performed on the T1+T1c+T2 combination using the “sym1” wavelet type and 2-fold cross-validation. While the SVM kernel parameter had a default value of “RBF” in the preliminary classification stage, it was changed to “linear” in the final classification stage. After the kernel change, classification accuracy improved. The obtained classification results are presented in the Table 3.

https://doi.org/10.56038/oprd.v2i1.239

Table 3: The final classification result

Com-bination	Data	Wavelet Type	k-fold	Metrics (%) (mean ± std)					
				SEN	SPE	ACC	PRE	F-score	AUC
Triple	T1 + T1c + T2	sym1	2	95,23±5,4	78,81±14,6	90,89±7,9	92,59±5,2	93,89±5,3	87,02±10,1

Table 3 indicates that the best classification accuracy increased to 90.89% from 90.17% after kernel parameter change. This mean if any other classification process is implemented on the best data combination, the classification accuracy may be increased more. The scheme of the proposed method is presented in Figure 3.

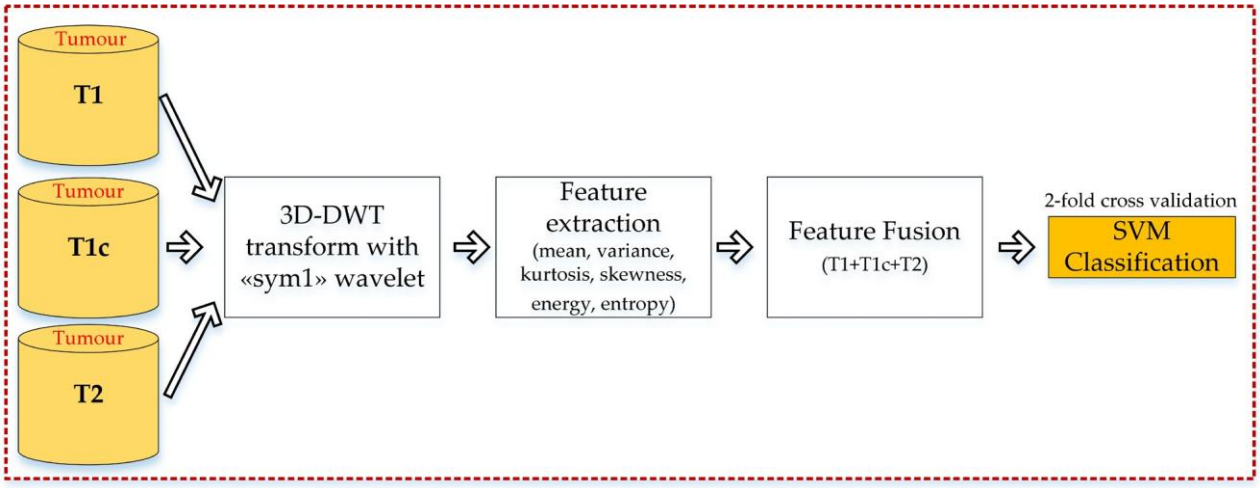

Figure 3: The proposed brain tumour classification method

4. Discussion and Conclusion

This study investigated the classification of brain tumours using support vector machine (SVM) with feature sets obtained from four different MRI modalities (FLAIR, T1, T1c, and T2). The results showed that SVM is an effective tool for classifying brain tumours, achieving an overall accuracy of up to 90.89% with the T1+T1c+T2 combination and the "sym1" wavelet type. The results also indicated that the type of wavelet used plays an important role in the performance of the SVM classifier, as different wavelets yielded different classification results. In the final classification stage, only the phase combination, wavelet type, and cross-validation type obtained in the preliminary classification stage were used. By changing the SVM kernel parameter from “RBF” to “linear”, the classification accuracy was improved. This suggests that the choice of kernel parameter is an important factor in the performance of the SVM classifier. The literature comparison is presented in the Table 4.

https://doi.org/10.56038/oprd.v2i1.239

Table 4: The literature studies

Paper	Data	Method	Accuracy (%)
[5]	BraTS 2017	Feature Extraction + Feature Ranking + Classification	90.17
[6]	BraTS 2012	DWT + CNN	98
	BraTS 2013		96
	BraTS 2015		100
	BraTS 2018		97
[8]	BraTS 2015	VGG16 + SVM	91.38
		AlexNet + SVM	94.83
		ResNet50 + SVM	98.28
[9]	BraTS 2013	PSO + CNN	98.3
	BraTS 2015		97.8
	BraTS 2017		96.9
	BraTS 2018		92.5
This study	BraTS 2017	3D-DWT + SVM	90.89

The literature studies show that the proposed method has several limitations that need to be addressed in future work. Firstly, this study used a relatively small dataset of 285 brain tumour cases, which may not be representative of the full range of brain tumours. Secondly, this study only used 3D wavelet transform. It is possible that other feature extraction methods may yield better classification results. Lastly, while the results are promising, they have not yet been validated on an independent dataset.

In conclusion, this study demonstrates the potential of SVM with feature sets obtained from MRI modalities and wavelet transformations for the classification of brain tumours. Further research is needed to validate the findings on larger and more diverse datasets, and to explore the use of other machine learning methods for brain tumour classification.

References

[1] H. Li, A. Li, M. J. C. i. b. Wang, and medicine, "A novel end-to-end brain tumor segmentation method using improved fully convolutional networks," vol. 108, pp. 150-160, 2019.

[2] Y. Li, F. Jia, and J. J. A. i. i. m. Qin, "Brain tumor segmentation from multimodal magnetic resonance images via sparse representation," vol. 73, pp. 1-13, 2016.

[3] M. Soltaninejad *et al.*, "Automated brain tumour detection and segmentation using superpixel-based extremely randomized trees in FLAIR MRI," vol. 12, pp. 183-203, 2017.

[4] B. J. J. o. M. Ural and B. Engineering, "A computer-based brain tumor detection approach with advanced image processing and probabilistic neural network methods," vol. 38, pp. 867-879, 2018.
[5] H. Koyuncu, M. Barstuğan, M. Ü. J. M. Öziç, B. Engineering, and Computing, "A comprehensive study of brain tumour discrimination using phase combinations, feature rankings, and hybridised classifiers," vol. 58, pp. 2971-2987, 2020.
[6] J. Amin, M. Sharif, N. Gul, M. Yasmin, and S. A. J. P. R. L. Shad, "Brain tumor classification based on DWT fusion of MRI sequences using convolutional neural network," vol. 129, pp. 115-122, 2020.
[7] J. Amin, M. Sharif, M. Raza, T. Saba, and A. Rehman, "Brain tumor classification: feature fusion," in *2019 international conference on computer and information sciences (ICCIS)*, 2019, pp. 1-6: IEEE.
[8] S. Kuraparthi *et al.*, "Brain Tumor Classification of MRI Images Using Deep Convolutional Neural Network," vol. 38, no. 4, 2021.
[9] M. I. Sharif, J. P. Li, M. A. Khan, and M. A. J. P. R. L. Saleem, "Active deep neural network features selection for segmentation and recognition of brain tumors using MRI images," vol. 129, pp. 181-189, 2020.
[10] B. H. Menze *et al.*, "The multimodal brain tumor image segmentation benchmark (BRATS)," vol. 34, no. 10, pp. 1993-2024, 2014.
[11] S. Bakas *et al.*, "Advancing the cancer genome atlas glioma MRI collections with expert segmentation labels and radiomic features," vol. 4, no. 1, pp. 1-13, 2017.
[12] S. Bakas *et al.*, "Identifying the Best Machine Learning Algorithms for Brain Tumor Segmentation," vol. 10, 2018.
[13] N. Aggarwal, B. Rana, R. J. I. J. o. I. S. Agrawal, and Technology, "3d discrete wavelet transform for computer aided diagnosis of A lzheimer's disease using t1-weighted brain MRI," vol. 25, no. 2,pp. 179-190, 2015.
[14] Z. Chen, R. J. C. M. I. Ning, and Graphics, "Breast volume denoising and noise characterization by 3D wavelet transform," vol. 28, no. 5, pp. 235-246, 2004.
[15] C. Yücelbas, S. Yucelbas, S. Ozsen, G. Tezel, S. Kuccukturk, and S. J. I. J. S. T. Yosunkaya, "Detection of sleep spindles in sleep EEG by using the PSD methods," vol. 9, no. 25, pp. 1-7, 2016.
[16] C. Yücelbaş *et al.*, "Automatic detection of sleep spindles with the use of STFT, EMD and DWT methods," vol. 29, pp. 17-33, 2018.
[17] M. A. Hearst, S. T. Dumais, E. Osuna, J. Platt, B. J. I. I. S. Scholkopf, and t. applications, "Support vector machines," vol. 13, no. 4, pp. 18-28, 1998.